Vol. 23, No. 3(2024) Poly24405
Revista Mexicana de Ingeniería Química

Cold plasma oligomerization in argon atmosphere from carvacrol: Product formation and characterization

Oligomerización por plasma frío en atmósfera de argón a partir de carvacrol: Formación y caracterización del producto

E.O. Martínez-Ruiz[1*]; J.A. González-López[1], C. G. Cuellar-Gaona[1], M. Á. González-López[2], J. R. Torres-Lubián[1], M.E. Treviño-Martínez[1], C. Gallardo-Vega[1], G. Soria-Arguello[1], M. G. Neira-Velázquez[1*]
[1]*Center of research in applied chemistry, C.P. 25294, Saltillo, Coah., Mexico.*
[2]*CONAHCYT-CIATEQ, C.P. 78395, San Luis Potosí, SLP, Mexico*
Received: August 21, 2024; Accepted: September 20, 2024

Abstract
Carvacrol, a monoterpenoid sourced from sustainable materials like oregano, has been studied for its oxidation into higher value compounds, such as thymoquinone or low molar mass derivatives, due to their applicability in epoxy resin synthesis. This oxidation process employs a range of catalysts, solvents and oxidizing agents. Cold plasma oligomerization of carvacrol in an argon atmosphere presents an alternative to catalytic methods. From 3 mL of carvacrol, 46 mg of solid product (Pcrol) were obtained, achieving a 35 ±0.5% selectivity. Surface examinations reveal a hydrophobic material with a meshed texture, while chemical characterization confirms the retention of functional groups, successful plasma oligomerization and provides insights into the reaction mechanism. The results identify Pcrol as an oligomer, and thermal analysis suggests it decomposes below 300 ±2.11 °C, likely due to its shorter oligomer chains.
Keywords: carvacrol; cold plasma; oligomer, sustainable, green chemistry.

Resumen
Carvacrol, un monoterpenoide obtenido de materiales sostenibles como el orégano, ha sido estudiado por su oxidación en compuestos de mayor valor, como la timoquinona o derivados de baja masa molar, debido a su aplicabilidad en la síntesis de resinas epoxi. Este proceso de oxidación implica el uso de diversos catalizadores, solventes y agentes oxidantes. Sin embargo, la oligomerización por plasma frío del carvacrol en una atmósfera de argón se presenta como una alternativa a los métodos catalíticos convencionales. A partir de 3 mL de carvacrol, se logró obtener 46 mg de un producto sólido (Pcrol), alcanzando una selectividad del 35 ±0.5%. Los análisis de la superficie revelaron la presencia de un material hidrofóbico con una textura entrelazada, mientras que la caracterización química confirmó la retención de los grupos funcionales, la exitosa oligomerización por plasma y proporciono información sobre el posible mecanismo de reacción. Los resultados identifican a Pcrol como un oligómero, y el análisis térmico sugiere que se descompone por debajo de los 300 ±2.11 °C, probablemente debido a la longitud de sus cadenas.
Palabras clave: carvacrol; plasma frío; oligómero, sustentabilidad, química verde.

*Corresponding author. *E-mail*: erickomr87@hotmail.com; guadalupe.neira@ciqa.edu.mx;
https://doi.org/10.24275/rmiq/Poly24405
ISSN:1665-2738, *issn-e*: 2395-8472

1 Introduction

In recent years, the development of organic polymer films has gained significant attention from the scientific community due to their numerous advantages (Arrieta-Almario *et al*., 2019). These materials are cost-effective, environmentally friendly, and chemically versatile, making them suitable for a wide range of applications (Nath & Bhuiyan, 2023). Carvacrol, a phenolic monoterpene found in plants of the Lamiaceae family, particularly in the essential oils of thyme and oregano (Origanum vulgare), exhibits notable antimicrobial and antioxidant properties (da Silva *et al*., 2023; Gaglio *et al*., 2021; Hajibonabi *et al*., 2023; Lopresti *et al*., 2021). These characteristics make carvacrol an attractive candidate to produce high value polymeric films.

Traditionally, the catalytic method has been the dominant approach for the oligo-polymerization of naturally derived monomers such as carvacrol, utilizing catalysts and oxidizing agents (Mohamed *et al*., 2023; Tessaro *et al*., 2022). However, this method has some drawbacks, including catalyst deactivation due to poisoning effects and the high costs associated with rare metal catalysts, which increase the overall expense of the oligomerization process. Plasma oligomerization presents an alternative technique that is efficient, clean, and biocompatible. This complex process involves free radicals and organic monomers, producing oligomers or polymers without the need for additional agents like catalysts or solvents (Michlíček *et al*., 2021). In plasma environments, an applied electric field generates a highly energetic and ionized atmosphere, which induces rapid movement of species, leading to the cleavage of monomer double bonds and their crosslinking, resulting in the formation of a polymer film on the substrate(Levien *et al*., 2023; Saramolee *et al*., 2021). The plasma process can be conducted under various electrode configurations, typically at low pressure and temperatures (Alba-Perez *et al*., 2020). Plasma oligomerization at atmospheric pressure is particularly suited for homogeneous and controlled oligomer production (Kopp *et al*., 2022).

Plasma oligomerization facilitates the recombination of monomeric units to create a randomly structured polymer, offering the advantage of rapid, solvent free deposition, often yielding branched structures (Alba-Perez *et al*., 2020). Plasma treated samples exhibit enhanced adhesion properties due to the incorporation of oxygen containing functional groups (Cuellar-Gaona *et al*., 2023; Levien *et al*., 2023). The properties of plasma polymer films are influenced by several parameters, including discharge power, monomer flow rate, polymerization time, substrate temperature, and reactor chamber pressure (Kabir *et al*., 2020).

Additionally, the use of noble gas plasma, especially argon (Ar), is noteworthy due to the presence of metastable species such as Ar^* and Ar^+ within the plasma phase. These species can optimize the oligomerization by modifying reaction dynamics (Wróbel *et al*., 2001).14 Argon plasma treatment can produce highly crosslinked surfaces with good mechanical properties without altering the chemical composition (Farr, 2023; Queiroz *et al*., 2014).

The primary objective of this study is to investigate the cold plasma oligomerization of carvacrol, a monoterpenoid derived from sustainable sources like oregano, as a viable alternative to traditional catalytic methods. This research aims to conduct plasma oligomerization of carvacrol in an argon atmosphere, quantify the selectivity of the resulting oligomer (Pcrol), and thoroughly characterize its surface properties, chemical composition, and thermal behavior. A key focus is to elucidate the structure of the formed oligomer and propose potential mechanisms underlying its formation. Furthermore, this study seeks to assess the thermal stability of Pcrol, particularly in terms of its crosslinked and hydrophobic nature.

It is crucial to highlight that plasma polymerization typically results in highly crosslinked polymers with good adhesion to the substrate. However, this study's unique aspect is the generation of low molecular weight polymers that are completely soluble and have a more controlled chemical structure compared to conventional plasma polymer coatings. In standard plasma polymerization, the high degree of crosslinking often makes it difficult to control the polymer's chemical structure, and some functional groups may be lost due to the plasma energy applied.

2 Experimental section

2.1 Plasma oligomerization of carvacrol

In Figure 1, the experimental setup consisted of a cylindrical glass vessel (1.65 L) equipped with stainless steel caps and a copper wire loop located around the body of the cylindrical vessel, one of the ends of the copper wire was connected to the plasma generator. The plasma reactor was linked to a 13.56 MHz radio frequency (RF) generator through an impedance-matching device (model AT-6 Automatic Matching Network). For maintaining a vacuum environment, a vacuum pump (Maxima C Plus, Fisher Scientific^{TM}) was employed. To monitor the vacuum pressure within the reactor, a single channel ACS 2000 controller indicator by Alcatel Vacuum Technology was employed. For the plasma oligomerization process, 3 mL of carvacrol (with a purity of 98% was used, Sigma Aldrich) was

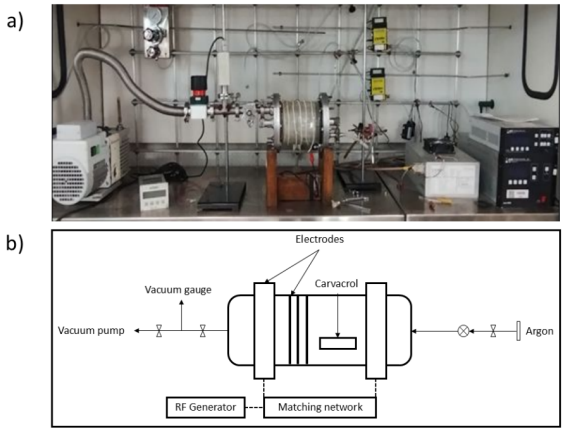

Figure 1. Experimental plasma reactor (a)) and plasma reactor scheme (b)).

introduced into a petri dish placed inside the plasma reactor. Plasma oligomerization was carried out in an argon atmosphere at 20 W for a duration of 40 minutes. Prior to the oligomerization process, the plasma reactor chamber was evacuated to a base pressure of 100 Pa. After the plasma oligomerization, the resulting oligomer (Pcrol) was recovered using a spatula (to remove it from the coverslip) and subsequently prepared for further characterization.

2.2 *Chemical characterization of Pcrol*

In this study, we conducted a chemical characterization of a Pcrol, revealing insights about its structural and compositional attributes.

2.2.1 *Nuclear magnetic resonance (NMR)*

Proton and carbon 13 nuclear magnetic resonance (^{1}H NMR and ^{13}C) spectra of the Pcrol and carvacrol were acquired under ambient conditions using a 400 MHz Bruker Avance III HD 400 NMR spectrometer equipped with a 5 mm multinuclear BBI decoupling probe featuring Z gradient functionality. Chemical shifts (expressed in ppm) were calibrated relative to the residual non deuterated chloroform signal (originating from $CDCl_3$) and employed as an internal reference in NMR spectroscopy.

2.2.2 *Matrix assisted laser desorption ionization time of flight mass spectrometry (MALDI-TOF-MS)*

The analysis involved mass spectrometry using a Bruker Autoflex SPEED MALDI-TOF-MS system, featuring a smart beam laser of 200 Hz frequency and a 337 nm wavelength. The experimental components included 2,5-Dihydroxybenzoic Acid (DHB) as the matrix, silver trifluoroacetate (Ag-TFA) as the cationizer, and Pcrol as the target sample. These were combined in a molar ratio of 3:1:0.1, and 1 μL aliquot of this mixture was deposited on a stainless-steel target plate, which was then air dried before introduction into the ionization chamber. The MALDI-TOF- MS was operated in positive reflector mode for ion detection, with the ion source 1 set to 19.67 kV, the ion source 2 to 18.03 kV, and the lens voltage at 7.31 kV. The mass scanning range was between 600 and 4500 m z $^{-1}$. Data acquisition involved averaging over 1000 laser pulses, with the laser power meticulously adjusted to slightly above the ionization threshold.

2.2.3 *Gel permeation chromatography (GPC)*

The determination of molar mass distribution of Pcrol was carried out through gel permeation chromatography using an Agilent series 1100 system, incorporating two sequential PLGel mixed C columns (5μm, 300 x 7.5mm), suitable for a molecular weight range of 200 to 3x10^{6} g mol^{-1}. Refractive index detection was employed at 40 °C. Tetrahydrofuran (THF) was used as the mobile phase. The Pcrol samples were prepared at a concentration of 5 mg mL^{-1} and filtered prior to injection into the chromatography system. The column temperature was consistently maintained at 40 °C ± 1 °C. Calibration for molecular weight assessment was achieved using a polystyrene standard calibration curve.

2.2.4 *Attenuated total Reflectance Fourier transform infrared (ATR-FTIR)*

A Thermo Scientific ATR-FTIR system (Nicolet IS 50 ATR) was used to obtain the Pcrol and carvacrol infrared spectra. Once the Pcrol was precipitated from the gas phase and removed with a scalpel from the plasma reactor, this sample was used for the FTIR measurement. To obtain the spectra, 100 scans were performed at a resolution of 4 cm^{-1}.

2.2.5 *Thermal gravimetric analysis (TGA)*

Thermogravimetric analysis of monomer and Pcrol was executed with a TGA-Q500-V6.7 instrument, utilizing open aluminum pans within a controlled dry nitrogen atmosphere (with a nitrogen flow rate of 100 cm^{3} min^{-1}). Approximately 5 mg of sample were used in each case. Temperature profiling involved a gradual ramp up from room temperature to 500 °C, with a heat rate of 10 °C min^{-1}.

2.2.6 *Differential Scanning Calorimetry (DSC)*

The DSC evaluation of monomer and Pcrol was conducted using a TA Instruments 2500. The heating protocol involved a rate of 20 °C min^{-1}, ranging from 30 to 175 °C. For this analysis, around 5 mg of the sample were allocated in an aluminum pan.

2.3 Morphological characterization of Pcrol

In this study, it was investigated the morphological characteristics of a synthesized Pcrol, employing state-of-the-art microscopic and analytical techniques. The morphological characterization elucidates the physical structure of the Pcrol.

2.3.1 Scanning electron microscopy (SEM)

Photographs of Pcrol were obtained utilizing the JEOL 6000 Scanning Electron Microscope (SEM). Before SEM analysis, the samples with Pcrol were previously mounted on aluminum *stubs* and coated with a 10 nm layer of silver by using a plasma sputtering system.

2.3.2 Static water contact angle (WCA)

The static water contact angle (WCA) of Pcrol was determined using the sessile drop method. The measurement was conducted with a ramé-hart apparatus (model 100-00), and the WCA images were acquired and analyzed using an Image J software. For image acquisition, 2 μL of milli-Q water was gently dispensed onto the sample surface manually.

2.4 Statistical analysis

Every experiment was conducted with at least three independent repetitions, each using a unique batch of random samples produced from different plasma oligomerization runs. The statistical evaluations were performed in Python (programming language), utilizing a one way ANOVA coupled with the Tukey-Kramer test. Results were considered statistically significant when the p-value fell below the 0.05 threshold.

3 Results and discussion

3.1 Plasma oligomerization process

In the literature, the catalytic method emerges as a predominant technique for oligomerizing monomers of natural origin like carvacrol, one alternative to the catalytic processes is the plasma oligomerization (Fridman *et al*., 2004; Özen *et al*., 2024). This technique offers an alternative approach for such natural compound oligomerizations. The exploration of plasma from noble gases with a focus on argon, is noteworthy due to the presence of metastable species within the argon plasma phase, like Ar^* (Fridman, 2008). These species can potentially modify the reaction dynamics, optimizing the oligomerization process in certain contexts. When 3 mL of carvacrol were subjected to the specified conditions in section

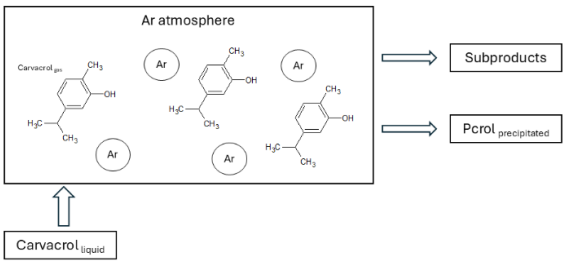

Figure 2. Schematic of the migration process of liquid carvacrol to the gas phase.

2.1 over a 40-minute duration, 46 ±1 mg of a solid product (plasma oligomer; Pcrol) were obtained. In the determination of selectivity as outlined in equation 1, the oligomerization reaction was executed within the gas phase environment of the system, under an argon atmosphere. The reaction process schematic is depicted in Figure 2. Notably, the calculated molar ratio (MR) carvacrol : argon was established at 1.4.

The quantification of carvacrol transitioning from the liquid to the gas phase (Δcrol) was achieved by assessing the weight change of the liquid carvacrol, comparing its initial mass to the residual mass after a 40-minute duration. This calculation yielded a Δcrol value of 132.43 ±7 mg. The selectivity of Pcrol was determined using the eq. (1).

$$\%S_{Pcrol} = \left[\frac{Pcrol_{Obtained}}{(\Delta_{crol})}\right] * 100 \qquad (1)$$

Where $\%S_{Pcrol}$ is the percent of Pcrol selectivity, $Pcrol_{obtained}$ is the total amount of Pcrol obtained in the process, Δcrol is the amount of carvacrol that migrates from the liquid phase to the gas phase, resulting in a selectivity of 35 ±0.5%. This selectivity value is comparable to that reported in the literature for carvacrol oligomerization processes by catalysis (Tessaro *et al*., 2022).

In the realm of carvacrol polymerization, catalytic systems affiliated with the poly(phenylene oxide) (PPO) family have been scrutinized. Notably, the employment of manganese porphyrin catalysts for the oxidation of carvacrol yields polymers characterized by low molecular weights. This phenomenon aligns with the findings presented in several recent studies. It has been observed that variables such as solvent choice, oxidant, and catalyst significantly influence both, the conversion efficiency and the specificity of product formation (Da Silva *et al*., 2017; Meireles *et al*., 2021; Tessaro *et al*., 2022). These factors may introduce economic and safety considerations, particularly due to solvent use and potential catalyst poisoning. Moreover, these systems are inherently complex, necessitating intricate design and operational strategies for product purification (Günay *et al*., 2016; Tessaro *et al*., 2022). Conversely, plasma based systems offer a distinct advantage by obviating the need for solvents and catalysts. This

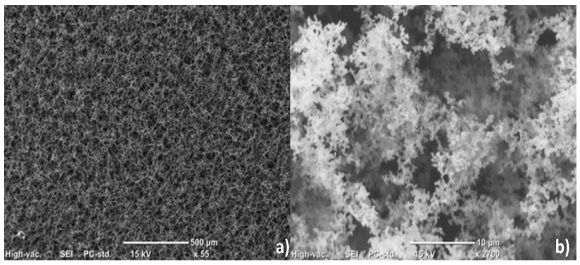

Figure 3. SEM images of Pcrol, scale bar of a) 500 μm and b) 10 μm.

approach potentially reduces environmental impact, energy consumption, and safety hazards. Furthermore, the absence of solvents simplifies the purification process, eliminating the necessity for extensive separation protocols. The oligomers produced via plasma technology exhibit promising applications, particularly in domains requiring materials that are both hydrophobic and thermally stable (Gazzotti *et al*., 2020; Günay *et al*., 2016; Tessaro *et al*., 2022).

3.2 Scanning electron microscopy

The images obtained by SEM for Pcrol, displayed in Figure 3a, reveal a uniform and consistent composition, characterized by a net-like texture reminiscent of a mesh, with a distribution of interspersed pores within the structures, this feature could be ideal for applications requiring a matrix for the controlled release of active compounds (Kwok *et al*., 1999). On the other hand, Figure 3b, allows for the distinction that the particle conformation is granular, with some notable agglomerations. The network texture with pores is maintained, which exhibits a size range close to 10 μm. SEM images from films fabricated using atmospheric plasma derived from carvacrol on steel discs are reported. These films exhibited holes encircled by clusters of particles varying in size. It is hypothesized that these variations in particle size may be attributed to plasma discharges, which are inherently filamentary in nature and a distinctive feature of cold plasma (Getnet *et al*., 2020). The material exhibited a WCA of 115 ±1.2°, allowing the material to be classified as hydrophobic. Similar polymeric materials are used in medical applications, as one of the stages in the mechanisms responsible for antimicrobial activity involves preventing the initial adhesion of bacteria on surfaces. This is achieved through the development of hydrophobic materials (Chan *et al*., 2016).

3.3 Nuclear magnetic resonance

Figure 4 presents the ^{1}H NMR spectra for both, the carvacrol monomer and the Pcrol oligomer. In the monomer spectrum, distinct signals are evident, representing the protonic entities within the carvacrol

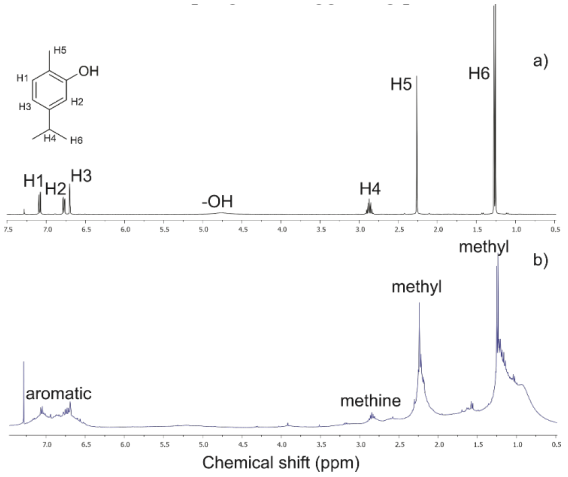

Figure 4. ^{1}H NMR spectrum of a) carvacrol and b) Pcrol in $CDCl_3$ (400 MHz, TMS) at 25 °C.

structure. The protons of the methyl groups (H5 and H6) exhibit signals at 2.25 and 1.22 ppm, respectively. The signal for the methine proton (H4) appears at 3.3 ppm. The aromatic ring protons of carvacrol, specifically those represented by H1, H2, and H3, display signals at 2.17, 6.57, and 6.79 ppm, in that order. Additionally, a subtle signal at 4.8 ppm, attributed to the carvacrol OH group is observed. Upon examining the spectra from the oligomerization of carvacrol, noticeable broadening with minor shifts in the protonic signals is apparent, noticeable signal of the presence of an oligomer. The spectra of the Pcrol batches reveal sharp signals, suggesting potential residual carvacrol within the oligomer.

The lack of OH groups in the Pcrol spectrum indicates a potential site for oligomerization via the removal of H^+ from that group (Günay *et al*., 2016; Tessaro *et al*., 2022). Due to their extended lifetimes relative to radiative processes, atoms and molecules in electronically excited metastable states are capable of accumulating sufficient discharge energy, thereby playing a significant role in the kinetics of various chemical reactions within plasma environments. These metastable excited particles may dissipate their energy not solely through radiative means but also through a range of collisional relaxation mechanisms. The excitation energies of metastable states, such as Ar^*, can be notably low (occasionally less than 1 eV), resulting in their high concentrations in electric discharges, as observed in the system studied in this work. The participation of Ar^* in the reaction mechanism might account for this, as illustrated in the reactions shown in Figure 5 (Fridman, 2008; Fridman *et al*., 2004). Cold plasmas, even at low temperatures, have the capability to generate energetic species that can catalyze chemical reactions which are challenging or unattainable using conventional chemical routes. Among the energetic species produced, the methyl radical (CH_3) serves as a notable example. Upon formation of the phenolic radical, it can subsequently

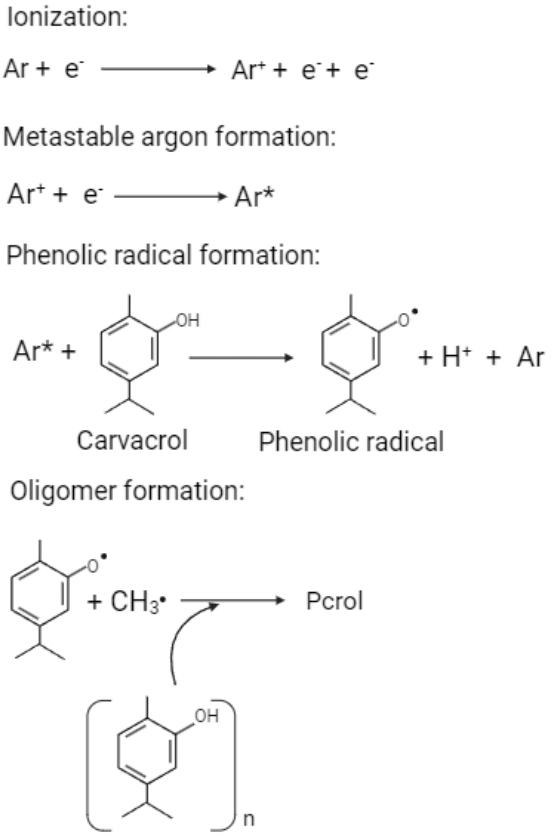

Figure 5. Potential mechanism pathway involving argon in the cold plasma oligomerization of carvacrol.

give rise to the methyl radical (CH_3). Methyl radicals are typically formed in the plasma phase when hydrocarbons are involved, such radicals are known to trigger the oligomerization processes (Fridman, 2008; Tessaro *et al*., 2022).

Figure 6 displays the ^{13}C NMR spectra for the carvacrol monomer (Figure 6a) and the Pcrol oligomer (Figure 6b). Carbon signals from the aromatic rings of Pcrol (C1 through C6) appear at 153.7, 148.4, 130.8, 120.9, 118.6, and 113 ppm, respectively. The methyl group carbons, C8 and C9, which appear at 24 and 15.3 ppm, respectively, and the methine carbon (C7) is discernible at 33.7 ppm. The Pcrol spectrum shows a notable broadening in its carbonic signals when juxtaposed with carvacrol, indicative of oligomer characteristics (Quirk *et al*., 2004; Swanson *et al*., 2021). When benchmarked against literature values, subtle deviations are evident in the Pcrol signals: 150.34, 137.11, 127.20, 119.02, and 116.9 ppm for C1 through C6 carbons; 22.9 and 16.07 ppm for the methyl group carbons (C8 and C9); and 27.11 ppm for the methine carbon (Tessaro *et al*., 2022). These deviations likely stem from the emergence of a branched oligomer structure, typical of plasma oligomerization processes (Kinmond *et al*., 2005).

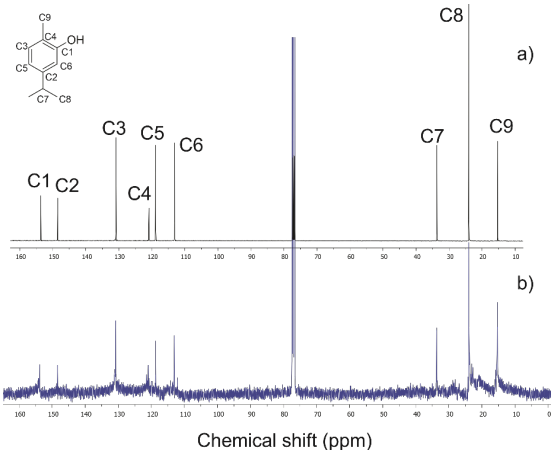

Figure 6. ^{13}C NMR spectrum of a)carvacrol and b)Pcrol in $CDCl_3$ (400 MHz, TMS) at 25 °C.

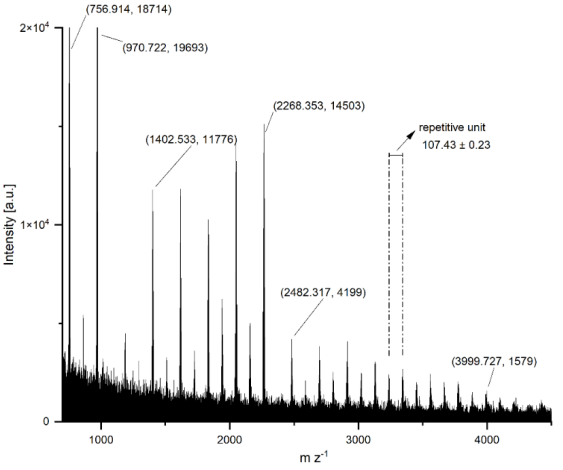

Figure 7. MALDI-TOF Spectrum of Pcrol.

3.4 Matrix assisted laser desorption ionization time of flight mass spectrometry

In Figure 7 is showed MALDI-TOF-MS spectrum of carvacrol, it is possible to observe regularly spaced peaks in the spectrum indicating the presence of repeating units in the oligomer chain Pcrol (Kinmond *et al*., 2005; Quirk *et al*., 2004). The difference in m z^{-1} values between adjacent peaks was close to 107 g mol^{-1}. This could suggest the detachment of the isopropyl group from the molecule of carvacrol during plasma oligomerization process.

As in the previously discussed NMR results, there is no evidence of the detachment of the isopropyl group from the aromatic ring of the carvacrol molecule. A possible explanation is the decomposition of the molecule through electronic impact in a stage of ionization, followed by fragmentation, and finally, its regeneration as described in Figure 8 (Fridman, 2008; Fridman *et al*., 2004; Günay *et al*., 2016; Tessaro *et al*., 2022). A possible explanation for

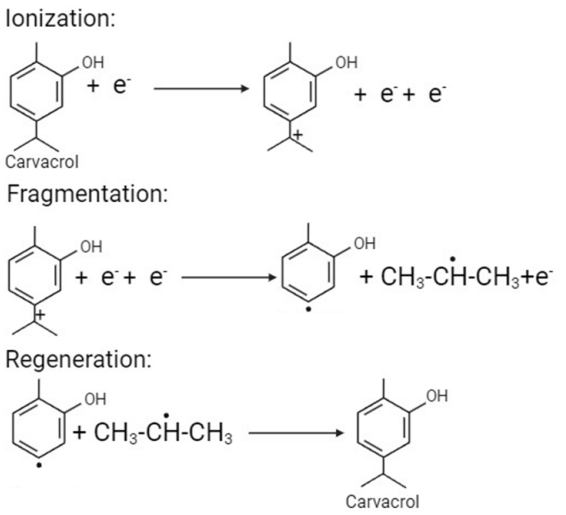

Figure 8. Potential mechanism pathway of ionization and regeneration of carvacrol during the plasma oligomerization process of carvacrol.

the regeneration phenomenon lies in the variation of electron concentration as a function of the electric field within the reactor, which exhibits a non-homogeneous distribution (Vafeas *et al*., 2020). This distribution could enhance initiation and fragmentation processes in regions with more intense electric fields (near the electrodes), while species regeneration would be favored in areas with weaker electric fields (farther from the electrodes). This hypothesis is further supported under vacuum conditions, where interference from other molecules is minimized, allowing for more precise control over the reactive species generated (Fridman, 2008). However, further studies are needed to validate this hypothesis.

In the spectrum, a dominant peak was evident between 750 and 970 m z^{-1}. This was succeeded by a moderately intense region from 1400 to 2270 m z^{-1} and ended with a fainter region spanning from 2450 to 4000 m z^{-1}. The m z^{-1} values identified suggest that Pcrol is an oligomer. These findings align with the average molar mass (Mw) of the oligomer associated with the main peak deduced from GPC, registering at 1175 g mol^{-1}. With a high value of polydispersity index (PDI = 1.99±0.1), there was a notable range in chain lengths, reinforcing the observations made in the MALDI-TOF spectrum, the observations align with previously reported findings in the literature, highlighting that polydispersity index (PDI) values, in the absence of thymoquinone production within PPO frameworks, exhibit markedly high polydispersity (PDI > 1.8) (Gul *et al*., 2022). In the field of polymer science, it is generally desirable to achieve polydispersity index values close to 1 to ensure homogeneity in the mechanical properties of the material. However, in the case of low molecular weight compounds belonging to the poly(phenylene oxide) family, such as the synthesized Pcrol, higher polydispersity is favored for their applicability in the synthesis of epoxy resins(Galizia *et al*., 2013; Hwang *et al*., 2008). Meanwhile, achieving monodispersity in polymers, where the polydispersity index is 1 or very close to 1, poses significant challenges. Typically, polymers synthesized in the laboratory exhibit a degree of polydispersity, and plasma synthesized polymers are not the exception. The inherent nature of the polymerization process results in the formation of polymer chains of varying lengths. This variability arises from the generation of polymer radicals of different sizes that interact and collide with others, leading to a diverse array of chain lengths within the final polymer product. Consequently, the specific mechanism of polymerization makes it exceedingly difficult to produce polymer chains of a uniform size. Therefore, in this study, we obtained polydisperse oligomers. Furthermore, in plasma driven systems that incorporate argon and hydrocarbons, a notable characteristic is the emergence of various reactive species (Fridman, 2008; Fridman *et al*., 2004; Martinez-Ruiz, 2017). These species, including free radicals such as $CH_3\cdot$ and CH_3-$CH_2\cdot$, along with other intermediate entities, may significantly contribute to the observed elevated polydispersity (PDI = 1.99 ±0.1). This phenomenon underscores the intricate dynamics of chain growth mechanisms within the polymerization process, suggesting a pivotal role for these reactive species in influencing the polydispersity of the resultant polymers. The PDI value appears to be linked to a mechanism known as chain growth oligomerization (McGuinness *et al*., 2008; Quirk *et al*., 2004). This correlation is supported by the suggested pathway and discussion (section 3.3) for the formation of the carvacrol oligomer. A technique for fractionating the polymer chains by size would be necessary to isolate the monomeric fractions of the material. We would need to employ various techniques, such as solvent based fractionation, along with molecular weight measurement methods, such as Gel Permeation Chromatography (GPC).

3.5 Attenuated Total Reflectance Fourier Transform Infrared Spectroscopy (ATR-FTIR)

ATR-FTIR serves as a crucial technique for the analysis of organic compounds, highlighting the functional groups present in a molecule (Herrera-González *et al*., 2019). By examining the molecular structure, it is possible to identify key functional groups, each with specific absorption bands in the ATR-FTIR spectrum (Figure 9) (Guerrero-Pérez *et al*., 2019). The absorption band corresponding to the hydroxyl (OH) group in phenol is apparent in the spectrum, positioned at 3375 cm^{-1} for Pcrol and 3324 cm^{-1} for carvacrol. The width and strength of this

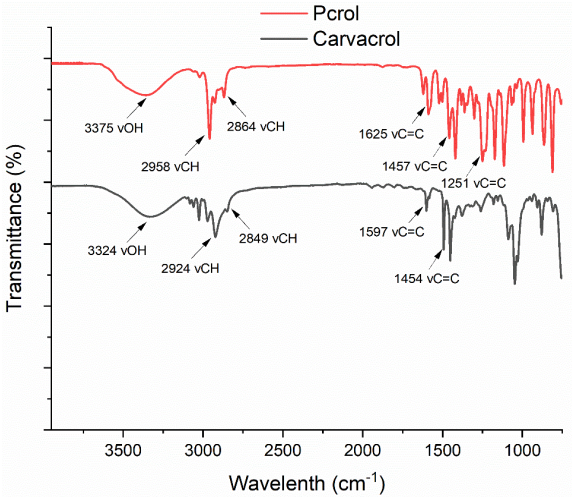

Figure 9. ATR-FTIR spectra of Pcrol and Carvacrol.

band arise from the hydrogen bonding typical of hydroxyl groups. Its vibration mode is a stretching motion, defined by the reciprocal movement of oxygen and hydrogen atoms along the O-H bond (França & Oliveira, 2022). The aromatic rings of the molecule present their inherent absorption bands. The stretching vibrations of the C=C bonds in the aromatic structure appear in the 1400-1650 cm^{-1} range. This movement illustrates the carbon atoms shifting back and forth along the C=C bond. Additionally, the aromatic C-H bond stretching results in a band close to 3030 cm^{-1}, with the hydrogen atoms coordinating with the bound carbon. Furthermore, the alkyl chain displays various vibrational modes in the spectrum. The stretching of the aliphatic C-H bonds, where hydrogen atoms move back and forth relative to the carbon, is observed between 2840-2960 cm^{-1}. Also, the bending vibration of the aliphatic C-H bond, indicating hydrogen movement at right angles to the bond, is discernible in the 1350-1470 cm^{-1} range (Thompson, 2018).

ATR-FTIR analysis of the oligomerized carvacrol revealed noteworthy features indicative of its structural changes post-oligomerization. Remarkably, the principal absorption bands corresponding to the functional groups inherent to carvacrol remain discernible in the oligomer's spectrum. This observation underpins the structural retention of key functional groups during the oligomerization process. One of the salient features in the spectrum of the oligomerized product is the preservation of the absorption band attributed to the hydroxyl (OH) group. This conservation suggests the potential presence of residual carvacrol in the reaction product, indicating that not all the monomers may have been fully incorporated into the oligomer matrix. Furthermore, a comparative analysis between the monomer and oligomer spectra unveils subtle but significant changes. The absorption bands in the oligomer spectrum are slightly broader than those of the monomer. This broadening is a hallmark

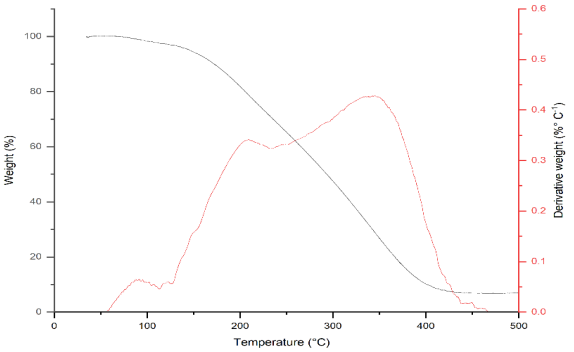

Figure 10. TGA thermogram and its derivate of Pcrol under N_2 atmosphere at a heating rate of 10 ºC min^{-1}.

characteristic of oligomerization, implying that the carvacrol has indeed undergone a transformation from its monomeric form to a more complex oligomeric structure (Ravve, 2012). A slight shift in most of the signals can be observed. In conclusion, the ATR-FTIR spectrum offers insights into the plasma oligomerization process of carvacrol.

3.6 Differential Scanning Calorimetry and Thermal gravimetric analysis

Figure 10 illustrates the thermal behavior of Pcrol. Initially, a minor weight reduction is observed below 100 ±2.11 °C, likely due to moisture evaporation (Tessaro *et al*., 2022; Yang *et al*., 2010). A significant weight loss becomes evident around 125 ±2.11 °C, continuing up to approximately 400 ±2.11 °C. The derivative analysis reveals that the thermal degradation process of Pcrol occurs via a two-step kinetics, with two prominent peaks at around 210±2.11 °C and 375±2.11 °C. This substantial decrease highlights the thermal degradation of Pcrol. The thermal degradation profile of Pcrol differs from those typically reported for poly(phenylene oxide), known for their high thermal stability, usually commencing around 400 ±2.11 °C. Pcrol, characterized as an oligomer with shorter chain lengths, exhibits a comparatively earlier onset of thermal decomposition (Tessaro *et al*., 2022; Yang et al., 2010). The primary degradation processes, including chain scission and bond disruption, predominantly occur within this temperature range. Beyond 300 ±2.11 °C, the weight loss stabilizes, indicating the completion of the main degradation phase (Chen *et al*., 2021; I Gi *et al*., 2024; Tessaro *et al*., 2022).

In Figure 11, the DSC thermogram (a representative sample of Pcrol is observed) exhibits an endothermic event near 65 ±2.11 °C, which might be interpreted as a glass transition (Tg). This suggests the presence of an oligomer with rigid characteristics (Tessaro *et al*., 2022). Subsequently, a stabilization in the DSC curve is observed, indicating that the sample has reached a stable thermal state, without

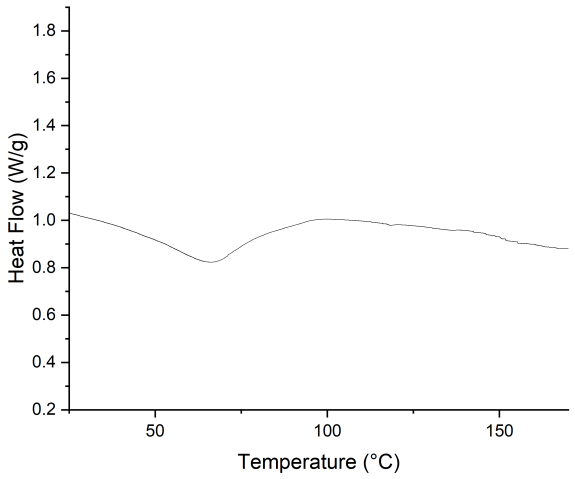

Figure 11. DSC curve from the oligomer of carvacrol.

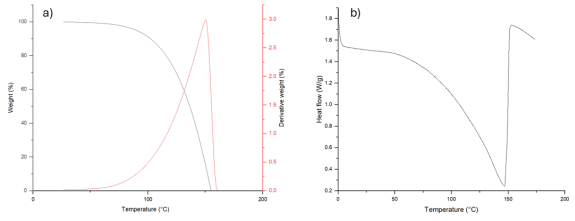

Figure 12. a) TGA thermogram and its derivate of Carvacrol under N_2 atmosphere at a heating rate of 10 ºC min^{-1}, b) DSC curve of carvacrol.

showing significant additional phase transitions within the examined temperature range.

Figure 12 illustrates a) the TGA thermogram and its derivative of carvacrol under a nitrogen atmosphere at a heating rate of 10 °C/min, and b) the DSC curve of carvacrol. Notable differences are evident when compared to the spectra of Pcrol, highlighting the impact of polymerization on the thermal properties and stability of the substances. The TGA thermogram of carvacrol (Figure 12a) demonstrates a gradual weight loss, beginning around 54 ±2.11 °C, indicative of thermal decomposition, whereas the carvacrol oligomer shows enhanced thermal stability, commencing its degradation at approximately 100±2.11 °C, as evidenced by higher decomposition temperatures. Furthermore, the DSC curves (Figure 12b) indicate thermal transitions that vary between the monomer and the oligomer. These variations include shifts in melting points and the appearance of new transitions, likely due to crosslinked structures or interactions among polymer chains.

Conclusion

Cold plasma oligomerization has proven to be an efficient technique for converting carvacrol into an oligomeric product (Pcrol), with a selectivity of 35 ±0.5%. NMR spectra have shown changes in protonic and carbonic signals, indicating the formation of an oligomeric structure in comparison to the carvacrol monomer. The absence of OH groups in the Pcrol spectrum is indicative of their involvement in the oligomerization site and the formation of phenolic radicals during the process. MALDI-TOF-MS and GPC analyses show the presence of repetitive units in the Pcrol chain. The m z^{-1} values identified for the oligomer chains indicate that Pcrol is an oligomer (1175 g mol^{-1}) with a polydispersity index of 1.99 ±0.1, which is consistent with the presence of chains of variable length. ATR-FTIR spectroscopy confirms the retention of the main functional groups of carvacrol in the oligomer. The appearance of broad bands in the absorption patterns between the monomer and oligomer reinforces the evidence of oligomerization. Thermogravimetric analysis (TGA) indicates that Pcrol exhibits earlier thermal degradation than other comparable polymers (degradation onset at 210 ±2.11 °C), suggesting a shorter chain length. These results illustrate that plasma oligomerization is a viable method for synthesizing oligomers from natural compounds such as carvacrol. The oligomerization of carvacrol presents a viable pathway for the synthesis of epoxy resins, capitalizing on the inherent chemical properties of this monoterpene. Carvacrol, which contains a phenolic hydroxyl group, offers suitable reactivity for functionalization, allowing the generation of oligomeric structures capable of crosslinking within epoxy resin matrices. Furthermore, the oligomeric characteristics derived from carvacrol can significantly enhance the mechanical and thermal properties of the resins, adjusting their flexibility and heat resistance. In specific applications, epoxy resins enriched with carvacrol oligomers could exploit the antibacterial and fungicidal properties of the compound, making them particularly valuable in sectors like the medical and food industries, where resistance to microorganisms is required. This approach not only enhances the functionality of epoxy resins but also aligns polymer chemistry with the principles of green chemistry and environmental responsibility. However, further research is required to optimize the yield and efficiency of oligomerization, as well as to explore practical applications of the developed oligomer.

Acknowledgements

The authors wish to express their gratitude for the financial support received for this paper in the form of a postdoctoral fellowship (grant 347182) from the National Council for Humanities, Science, and Technology (CONAHCYT). They would also like to extend their thanks to M. García Zamora, G. Rodríguez Rojas, B. Reyes Vielma, G. Mendez

Padilla, Pablo Acuña Vázquez and H. Maldonado Textle for their invaluable technical assistance with several of the analytical methods employed in this study. Additionally, the authors are thankful for the insightful remarks provided by O. Pérez Camacho from the Research Center in Applied Chemistry (Centro de Investigación en Química Aplicada) concerning this research.

Abbreviations

ATR-FTIR, Attenuated Total Reflection Fourier Transform Infra-Red; **DSC**, Differential Scanning Calorimetry, **GPC**, Gel Permeation Chromatography; **MALDI-TOF-MS**, Matrix Assisted Laser Desorption Ionization Time Of Flight Mass Spectrometry; **MR**, Molar Ratio; **NMR**, Nuclear Magnetic Resonance; **Pcrol**, synthesized oligomer; **PDI**, polydispersity index; **PPO**, poly(phenylene oxide); **SEM**, Scanning Electron Microscopy; **TGA,** Thermal Gravimetric Analysis, **THF,** Tetrahydrofuran; **WCA**, Water Contact Angle.

References

Alba-Perez, A., Jayawarna, V., Childs, P. G., Dalby, M. J., & Salmeron-Sanchez, M. (2020). Plasma polymerised nanoscale coatings of controlled thickness for efficient solid-phase presentation of growth factors. *Materials Science and Engineering: C*, *113*, 110966. https://doi.org/10.1016/J.MSEC.2020.110966

Arrieta-Almario, A. A., Mendoza-Fandiño, J. M., & Palencia-Luna, M. S. (2019). Composite material elaborated from conducting biopolymer cassava starch and polyaniline. *Revista Mexicana de Ingeniería Química*, *19*(2), 707–715. https://doi.org/10.24275/rmiq/Mat765

Chan, Y. W., Siow, K. S., Ng, P. Y., Gires, U., & Yeop Majlis, B. (2016). Plasma polymerized carvone as an antibacterial and biocompatible coating. *Materials Science and Engineering: C*, *68*, 861–871. https://doi.org/10.1016/j.msec.2016.07.040

Chen, Y.-H., Chuang, E.-Y., Jheng, P.-R., Hao, P.-C., Hsieh, J.-H., Chen, H.-L., Mansel, B. W., Yeh, Y.-Y., Lu, C.-X., Lee, J.-W., Hsiao, Y.-C., & Bolouki, N. (2021). Cold-atmospheric plasma augments functionalities of hybrid polymeric carriers regenerating chronic wounds: In vivo experiments. *Materials Science and Engineering: C*, *131*, 112488. https://doi.org/10.1016/j.msec.2021.112488

Cuellar-Gaona, C. G., Ibarra-Alonso, M. C., Narro-Céspedes, R. I., Neira-Velázquez, M. G., Dávila-Medina, M. D., Zugasti-Cruz, A., Esparza-González, S. C., Sáenz-Galindo, A., & Martínez-Ruiz, E. O. (2023). Enhancing biocompatibility and antimicrobial efficacy through plasma technology modification of chitosan/Rosmarinus officinalis hydrogels. *Revista Mexicana de Ingeniería Química*, *23*(1), 1–29. https://doi.org/10.24275/rmiq/Poly24171

da Silva, A. R. P., Costa, M. do S., Araújo, N. J. S., de Freitas, T. S., dos Santos, A. T. L., Gonçalves, S. A., da Silva, V. B., Andrade-Pinheiro, J. C., Tahim, C. M., Lucetti, E. C. P., & Coutinho, H. D. M. (2023). Antibacterial activity and antibiotic-modifying action of carvacrol against multidrug-resistant bacteria. *Advances in Sample Preparation*, *7*, 100072. https://doi.org/10.1016/j.sampre.2023.100072

Da Silva, V. S., Dos Santos Vieira, W. C., Meireles, A. M., Ucoski, G. M., Nakagaki, S., Idemori, Y. M., & DeFreitas-Silva, G. (2017). Biomimetic oxidation of cyclic and linear alkanes: high alcohol selectivity promoted by a novel manganese porphyrin catalyst. *New Journal of Chemistry*, *41*(3). https://doi.org/10.1039/c6nj03072f

Farr, N. T. H. (2023). Regulating the formation and extent of crazing through the application of argon plasma surface functionalisation. *Polymer Testing*, *128*, 108244. https://doi.org/10.1016/j.polymertesting.2023.108244

França, A. S., & Oliveira, L. S. (2022). FTIR Spectroscopy: Advances in Research and Applications. In A. S. França & L. S. Oliveira (Eds.), *FTIR Spectroscopy: Advances in Research and Applications*. Nova Science Publishers. https://doi.org/10.52305/GOJG7949

Fridman, A. (2008). Plasma Chemistry. In *Plasma Chemistry* (Vol. 9780521847353). Cambridge University Press. https://doi.org/10.1017/CBO9780511546075

Fridman, A., Fridman, A., Kennedy, L. A., & Kennedy, L. A. (2004). *Plasma Physics and Engineering*. CRC Press. https://doi.org/10.1201/9781482293630

Gaglio, R., Botta, L., Garofalo, G., Miceli, A., Settanni, L., & Lopresti, F. (2021). Carvacrol activated biopolymeric foam: An effective packaging system to control the development of spoilage and pathogenic bacteria on sliced

pumpkin and melon. *Food Packaging and Shelf Life*, *28*, 100633. https://doi.org/10.1016/J.FPSL.2021.100633

Galizia, M., Daniel, C., Guerra, G., & Mensitieri, G. (2013). Solubility and diffusivity of low molecular weight compounds in semi-crystalline poly-(2,6-dimethyl-1,4-phenylene)oxide: The role of the crystalline phase. *Journal of Membrane Science*, *443*, 100–106. https://doi.org/10.1016/j.memsci.2013.04.070

Gazzotti, S., Ortenzi, M. A., Farina, H., Disimino, M., & Silvani, A. (2020). Carvacrol- And Cardanol-Containing 1,3-Dioxolan-4-ones as Comonomers for the Synthesis of Functional Polylactide-Based Materials. *Macromolecules*, *53*(15). https://doi.org/10.1021/acs.macromol.0c01537

Getnet, T. G., da Cruz, N. C., Kayama, M. E., & Rangel, E. C. (2020). *Plasma Polymer Deposition of Neutral Agent Carvacrol on a Metallic Surface by Using Dielectric Barrier Discharge Plasma in Ambient Air* (pp. 716–725). Universidade Estadual Paulista (Unesp). https://doi.org/10.1007/978-3-030-43690-2_55

Guerrero-Pérez, M. O., Gregory, |, Patience, S., & Guerrero-Pérez, M. O. (2019). *Experimental methods in chemical engineering: Fourier transform infrared spectroscopy-FTIR*. https://doi.org/10.1002/cjce.23664

Gul, U., Khan, M. I., Madni, A., Sohail, M. F., Rehman, M., Rasul, A., & Peltonen, L. (2022). Olive oil and clove oil-based nanoemulsion for topical delivery of terbinafine hydrochloride: *in vitro* and *ex vivo* evaluation. *Drug Delivery*, *29*(1), 600–612. https://doi.org/10.1080/10717544.2022.2039805

Günay, T., Çimen, Y., Karabacak, R. B., & Türk, H. (2016). Oxidation of Thymol and Carvacrol to Thymoquinone with KHSO5 Catalyzed by Iron Phthalocyanine Tetrasulfonate in a Methanol–Water Mixture. *Catalysis Letters*, *146*(11), 2306–2312. https://doi.org/10.1007/s10562-016-1850-2

Hajibonabi, A., Yekani, M., Sharifi, S., Nahad, J. S., Dizaj, S. M., & Memar, M. Y. (2023). Antimicrobial activity of nanoformulations of carvacrol and thymol: New trend and applications. *OpenNano*, *13*, 100170. https://doi.org/10.1016/J.ONANO.2023.100170

Herrera-González, A. M., Caldera-Villalobos, M., Pérez-Mondragón, A. A., Cuevas-Suárez, C. E., & González-López, J. A. (2019). Analysis of Double Bond Conversion of Photopolymerizable Monomers by FTIR-ATR Spectroscopy. *Journal of Chemical Education*, *96*(8), 1786–1789. https://doi.org/10.1021/acs.jchemed.8b00659

Hwang, H., Hsu, S., & Wang, C. (2008). Synthesis and physical properties of low-molecular-weight redistributed poly(2,6-dimethyl-1,4-phenylene oxide) for epoxy resin. *Journal of Applied Polymer Science*, *110*(3), 1880–1890. https://doi.org/10.1002/app.28770

I Gi, C., Gan, S. N., & Ang, D. T.-C. (2024). Designing polymeric coating with low coefficient of friction for natural rubber glove application. *Journal of Industrial and Engineering Chemistry*, *132*, 496–506. https://doi.org/10.1016/j.jiec.2023.11.043

Kabir, H., Nasrin, R., Mahbubur Rahman, M., & Bhuiyan, A. H. (2020). Heat treatment effect on the structural, morphological, and optical properties of plasma polymerized furan-2-carbaldehyde thin films. *Results in Physics*, *16*, 103014. https://doi.org/10.1016/J.RINP.2020.103014

Kinmond, E. J., Coulson, S. R., Badyal, J. P. S., Brewer, S. A., & Willis, C. (2005). High structural retention during pulsed plasma polymerization of 1H,1H,2H-perfluorododecene: an NMR and TOF-SIMS study. *Polymer*, *46*(18), 6829–6835. https://doi.org/10.1016/j.polymer.2005.05.112

Kopp, D., Lackner, J. M., Kaindl, R., Elter, R., Stummer, M., Hinterer, A., Coclite, A. M., & Waldhauser, W. (2022). Low-friction, wear-protecting coatings on polymers by atmospheric pressure plasma spraying. *Surface and Coatings Technology*, *448*, 128930. https://doi.org/10.1016/J.SURFCOAT.2022.128930

Kwok, C. S., Horbett, T. A., & Ratner, B. D. (1999). Design of infection-resistant antibiotic-releasing polymers. *Journal of Controlled Release*, *62*(3), 301–311. https://doi.org/10.1016/S0168-3659(99)00105-4

Levien, M., Amin, I., Vicente de Paula Kodaira, F., & Weltmann, K. D. (2023). Direct grafting of microwrinkled hydrogels by atmospheric-pressure plasma polymerization: Going simple and environmentally friendly. *European Polymer Journal*, *198*, 112413. https://doi.org/10.1016/J.EURPOLYMJ.2023.112413

Lopresti, F., Botta, L., La Carrubba, V., Di Pasquale, L., Settanni, L., & Gaglio, R. (2021). Combining carvacrol and nisin in biodegradable films for antibacterial packaging applications. *International Journal of Biological Macromolecules*, *193*, 117–126. https://doi.org/10.1016/J.IJBIOMAC.2021.10.118

Martinez-Ruiz, E. O. (2017). *Partial oxidation of methane in a dielectric barrier discharge plasma milli-reactor*. https://doi.org/10.13039/501100005737

McGuinness, D. S., Suttil, J. A., Gardiner, M. G., & Davies, N. W. (2008). Ethylene Oligomerization with Cr-NHC Catalysts: Further Insights into the Extended Metallacycle Mechanism of Chain Growth. *Organometallics*, *27*(16), 4238–4247. https://doi.org/10.1021/om800398e

Meireles, A. M., Guimarães, A. S., Querino, G. R., Castro, K. A. D. de F., Nakagaki, S., & DeFreitas-Silva, G. (2021). Exploring manganese pyridylporphyrin isomers for cyclohexane oxidation: First-generation catalysts are better than third-generation ones. *Applied Organometallic Chemistry*, *35*(11). https://doi.org/10.1002/aoc.6400

Michlíček, M., Blahová, L., Dvořáková, E., Nečas, D., & Zajíčková, L. (2021). Deposition penetration depth and sticking probability in plasma polymerization of cyclopropylamine. *Applied Surface Science*, *540*, 147979. https://doi.org/10.1016/j.apsusc.2020.147979

Mohamed, H. O., Velisoju, V. K., Hita, I., Abed, O., Parsapur, R. K., Zambrano, N., Hassine, M. Ben, Morlanes, N., Emwas, A.-H., Huang, K.-W., & Castaño, P. (2023). Highly productive framework bounded Ni^{2+} on hierarchical zeolite from ethylene oligomerization. *Physical Science and Engineering*, *475*, 23955–26900. https://doi.org/10.1016/j.cej.2023.146077

Nath, S. D., & Bhuiyan, A. H. (2023). Charge carrier transport mechanism in plasma polymerized methyl acrylate thin films. *Thin Solid Films*, *786*, 140098. https://doi.org/10.1016/J.TSF.2023.140098

Özen, I., Demir, A., Bahtiyari, M. I., Wang, X., Nilghaz, A., Wu, P., Shirvanimoghaddam, K., & Naebe, M. (2024). Multifaceted applications of thymol/carvacrol-containing polymeric fibrous structures. *Advanced Industrial and Engineering Polymer Research*, *7*(2), 182–200. https://doi.org/10.1016/j.aiepr.2023.09.001

Queiroz, J. D. F. de, Leal, A. M. de S., Terada, M., Agnez-Lima, L. F., Costa, I., Pinto, N. C. de S., & Batistuzzo de Medeiros, S. R. (2014). Surface modification by argon plasma treatment improves antioxidant defense ability of CHO-k1 cells on titanium surfaces. *Toxicology in Vitro*, *28*(3), 381–387. https://doi.org/10.1016/J.TIV.2013.11.012

Quirk, R. P., Guo, Y., Wesdemiotis, C., & Arnould, M. A. (2004). Investigation of ethylene oxide oligomerization during functionalization of poly(butadienyl)lithium using MALDI-TOF MS and 1H NMR analyses. *Polymer*, *45*(10), 3423–3428. https://doi.org/10.1016/j.polymer.2004.03.022

Ravve, A. (2012). Principles of Polymer Chemistry. In *Principles of Polymer Chemistry, Third Edition*. Springer New York. https://doi.org/10.1007/978-1-4614-2212-9

Saramolee, P., Trubmusik, S., Sunthondecha, T., Nisoa, M., & Johns, J. (2021). Effect of plasma-polymerised acetylene-coated silica on the compound properties of natural rubber composites. *Heliyon*, *7*(10), e08120. https://doi.org/10.1016/J.HELIYON.2021.E08120

Swanson, W. B., Tabaczynski, D., Lis, D., Zurek, E., & Kozik, M. (2021). Direct experimental 31P 2D DOSY NMR evidence for oligomerization of transition-metal substituted polyoxotungstates in nonpolar solvents. *Polyhedron*, *204*, 115174. https://doi.org/10.1016/j.poly.2021.115174

Tessaro, P. S., Meireles, A. M., Guimarães, A. S., Schmitberger, B., Lage, A. L. A., Patrício, P. S. de O., Martins, D. C. da S., & DeFreitas-Silva, G. (2022). The polymerization of carvacrol catalyzed by Mn-porphyrins: obtaining the desired product guided by the choice of solvent, oxidant, and catalyst. *New Journal of Chemistry*, *46*(44), 21136–21147. https://doi.org/10.1039/D2NJ03171J

Thompson, J. M. (2018). *Infrared Spectroscopy*. Jenny Stanford Publishing. https://doi.org/10.1201/9781351206037

Vafeas, P., Papadopoulos, P. K., Vafakos, G. P., Svarnas, P., & Doschoris, M. (2020). Modelling the electric field in reactors yielding cold atmospheric–pressure plasma jets. *Scientific*

Reports, *10*(1), 5694. https://doi.org/10.1038/s41598-020-61939-7

Wróbel, A. M., Walkiewicz-Pietrzykowska, A., Hatanaka, Y., Wickramanayaka, S., & Nakanishi, Y. (2001). Oligomerization and Polymerization Steps in Remote Plasma Chemical Vapor Deposition of Silicon-Carbon and Silica Films from Organosilicon Sources. *Chemistry of Materials*, *13*(8), 2742–2742. https://doi.org/10.1021/cm012004o

Yang, Z., Peng, H., Wang, W., & Liu, T. (2010). Crystallization Behavior of Poly(e-caprolactone)/Layered Double Hydroxide Nanocomposites. *J Appl Polym Sci*, *116*, 2658–2667. https://doi.org/10.1002/app.31787